Photoenhanced Uptake of NO_2 by Pyrene Solid Films†

Marcello Brigante,‡ David Cazoir,‡ Barbara D'Anna,‡ Christian George,*,‡ and D. J. Donaldson*,§

University Lyon 1 and CNRS, UMR5256, IRCELYON, Institut de Recherches sur la Catalyse et l'Environnement de Lyon, Villeurbanne, F-69626, France, and Department of Chemistry, University of Toronto, 80 St. George Street, Toronto, Ontario, Canada M5S 3H6

Received: March 17, 2008; Revised Manuscript Received: May 26, 2008

We report uptake kinetics measurements of the heterogeneous reaction of gas phase NO_2 with solid films of pyrene. By using a coated flow tube equipped with several near-ultraviolet (UV) emitting lamps (range 300−420 nm), we examined the effect of actinic radiation on the heterogeneous loss kinetics of nitrogen dioxide. With atmospherically relevant concentrations of NO_2, (20−119 ppbv), the uptake ranged from below 10^{-7} in the dark to 3.5×10^{-6} under near-UV irradiation. Under illuminated conditions, the uptake coefficient decreased markedly with increasing gas-phase concentration, suggestive of a Langmuir−Hinshelwood-type surface reaction mechanism. The NO_2 reactivity was not a function of deposited Pyrene mass or of the relative humidity (in the range 10−89%) and depended linearly on the intensity of illumination. Gas-phase product analysis indicated that approximately 50% of the NO_2 loss could be accounted for by HONO and NO release. These experimental results are discussed along with a possible nitration mechanism.

Introduction

Atmospheric aerosol particles have been found typically to contain moderate-to-high fractions by mass of organic compounds. These may be biogenic or anthropogenic in origin, depending on the location and history of the individual particle. The recent and growing awareness of this has spurred a significant effort in understanding how organic compounds on particle surfaces influence water condensation there, how this changes as the particle becomes processed (i.e., oxidized) in the atmosphere, and how these processes influence the gas-phase composition in volumes containing such particles.[1] Another type of surface which contains a moderate mass fraction of organics and is exposed to the urban atmosphere is the coating on impervious surfaces in an urban environment (urban organic films or window grime).[2–5] Although such surfaces are not important in cloud formation (at least directly), the films can act as sequestering agents for any compounds associated with them[6] and also act as a substrate for chemical reaction,[7] in the same manner as particle surfaces. Such surface films contain many of the same organic compounds as aerosol particles,[5] including polycyclic aromatic hydrocarbons (PAHs); therefore, the heterogeneous oxidation processes are expected to be similar.

A large number of recent laboratory studies of processing have involved reactions of gas-phase ozone,[7–15] nitrogen dioxide,[8,16,17] or NO_3 radical[8,18] with a PAH sample, either adsorbed to a surface or as a solid film. Among these, the studies of ozone reactions with PAHs have provided the greatest amount of kinetic insight, because many of these[7,9–13,15] have spanned a wide range of ozone concentrations. These studies have shown that PAH ozonation follows a Langmuir−Hinshelwood mechanism,[19] in which ozone is in rapid equilibrium between the surface and the gas phase and reaction takes place between the adsorbed PAH and coadsorbed ozone. Although heterogeneous reactions of PAHs with nitrogen dioxide have been studied for 30 years,[16,17,20] there have been hardly any extensive kinetic studies over a range of gas-phase NO_2 concentrations published to date (a recent exception is the study of Arens et al.,[21] which focused on product formation).

Recently, a different type of heterogeneous reaction involving gas-phase NO_2 or O_3 has been reported,[22–26] in which the gas-phase reagent reacts more rapidly at the substrate surface when the latter is illuminated at wavelengths absorbed by various compounds present there. Enhanced loss of NO_2 has been reported on surfaces containing a number of known photosensitizers (i.e., benzophenone, catechol), as well as some PAHs (anthracene and perylene).[22] As well, humic acid films and particles[25] are found to give a photoenhanced heterogeneous NO_2 uptake. A significant production of HONO is measured in these experiments, amounting to 10−80% of the NO_2 loss, depending on the exact experimental conditions. Recently, photoenhanced uptake has been reported for ozone reacting with benzophenone-containing films, as well.[24]

The aim of the present work was to investigate the heterogeneous reaction of nitrogen dioxide on solid pyrene films and the possible role of photoenhancement in this reaction. We find that under atmospheric conditions, the reactive uptake of gas-phase NO_2 by solid pyrene films is considerably enhanced under illumination, compared to that measured in the dark. This enhancement amounts to a factor of 10 in the range of 20−119 ppbv of NO_2.

Experimental Section

The experiments were performed in a cylindrical illuminated flow tube apparatus made of Pyrex, which is described fully in Jammoul et al.[24] A mixture of NO_2 in N_2 was introduced to the flow tube at a total flow rate of 0.25 SLM via a movable injector of radius 0.3 cm. The NO_2 concentration at the exit of the flow tube was measured as a function of the gas-surface contact time, controlled by changing the position of the injector along the

† Part of the "Stephen R. Leone Festschrift".

* Corresponding authors. E-mail: Christian.George@ircelyon.univ-lyon1.fr and jdonalds@chem.utoronto.ca.

‡ University Lyon 1.

§ University of Toronto.

10.1021/jp802324g CCC: $40.75
Published on Web 08/06/2008

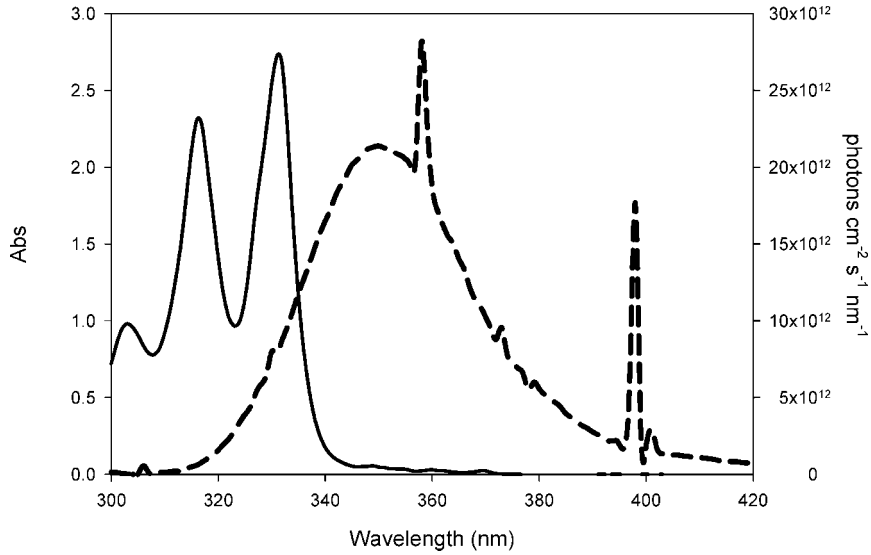

Figure 1. Spectral features of importance to the study. The dashed line with the right-hand axis shows the irradiance of four Cleo lamps in the range 300−420 nm (total flux intensity = 9.5×10^{14} photons cm^{-2} s^{-1}), and the solid line and the left-hand axis displays the absorbance spectrum of pyrene dissolved in methanol.

tube. The NO_2 exiting the tube was detected by using a THERMO 42C chemiluminescent analyzer for NO/NO_2 detection, in combination with a sodium carbonate denuder tube for removing HONO from the gas stream. A molybdenum catalyst reduces HONO and NO_2 to NO prior to chemiluminescent detection, so that NO, NO_2, and HONO are measured with equal analytical response. The sodium carbonate denuder tube (30 cm $\times$ 0.3 cm ID glass tube) may be either switched into the sampling line to measure the sum of the species NO and NO_2 or bypassed so that the chemiluminescence detector signal gives the sum of the species NO, NO_2, and HONO. The HONO concentration can therefore be expressed as the difference of the chemiluminescence detector signal without and with the carbonate denuder in the sampling line.[27] The NO concentration is obtained by bypassing the molybdenum converter.

Typical experimental conditions employed NO_2 abundances in the range of 20−119 ppbv ($5-29 \times 10^{11}$ molec cm^{-3}). All experiments reported here were conducted at a constant temperature of 283 ± 1 K, maintained by circulating thermostatted water through an outer jacket of the flow tube. The experiments were performed under atmospheric pressure, over a range of relative humidity (RH) from 10 to 90%. The RH in the flow tube was controlled by passing a stream of N_2 gas through a bubbler filled with deionized water thermostatted at the same temperature as the flow tube reactor, then mixing this in known proportion with the dry NO_2/N_2 flow. The humidity and the temperature of the gas flows were measured by using an SP UFT75 Sensor (Partners BV).

Surrounding the reactor were mounted four fluorescent lamps (Philips CLEO 20W) having a continuous emission in the 300−420 nm range. Figure 1 displays the measured spectral irradiance of the four lamps used during these experiments, as well as a UV−vis spectrum of pyrene in methanol solution to show the spectral overlap. The wavelength-dependent light flux reaching the solid film was measured[24] by putting an optical fiber coupled to spectrograph with CCD detector (Andor Fast Kinetics UV enhanced CCD and Shamrock spectrograph) inside the Pyrex flow tube and calibrating the resulting spectral intensities by using a reference deuterium lamp (DH-2000, Ocean Optics). Over the wavelength range 300−420 nm, a total flux of 9.5×10^{14} photons cm^{-2} s^{-1} was measured. Any output from the lamps with wavelengths shorter than ~300 nm is absorbed by the Pyrex walls of the flow reactor and therefore cannot contribute to the results described below.

Unless otherwise stated, solid films were prepared by depositing 250 μL of a solution of pyrene dissolved in methanol (24.7 mmol L^{-1}) on the inside walls of the flow tube, followed by evaporation of the solvent under a flow of dry N_2. We estimate that this amount of pyrene, if evenly deposited on the surface, amounts to about 370 molecular layers. The extent of coverage was modified by changing the amount of solution deposited; in the present work, we explored a range of pyrene surface densities of 0.2 −36.2 $\mu g/cm^2$.

All gases were taken directly from cylinders without further purification prior to use. High purity N_2 (99.9%) and NO_2 (1 ppmv in N_2; 99.0%) were both purchased from Alphagaz (France). The carrier gases passed into the flow reactor via digital mass flow controllers (Brooks) attached directly to the upstream end of the reservoir via Teflon tubing. Methanol was purchased from Merck (HPLC grade) and pyrene from ACROS Organics (98%); both were used as supplied

Kinetic Analysis

The NO_2(g) loss in the flow tube was measured as a function of injector position, which could be related to different gas/solid contact times by using the known total flow velocity. Each measurement at a different injector position was carried out by using a freshly prepared pyrene sample. Typically, experiments proceeded as follows, with the corresponding NO_2 concentrations shown in Figure 2. First, a constant flow of NO_2 was established, with the injector placed at the end of the flowtube, such that none of the pyrene-coated surface was exposed to the gas flow. This is indicated by region 1 in the figure. After the NO_2 concentration was steady, the injector was withdrawn a certain amount (at point 2) to expose some fraction of the pyrene-coated flow tube wall to the gas, and the flow was allowed to stabilize again. The NO_2 concentration difference between these two regions yields the loss under dark conditions. At point 3 on the figure, the lamps were turned, on and the signal was again allowed to stabilize. The NO_2 change here from region 1 gives the uptake under illumination. The signal

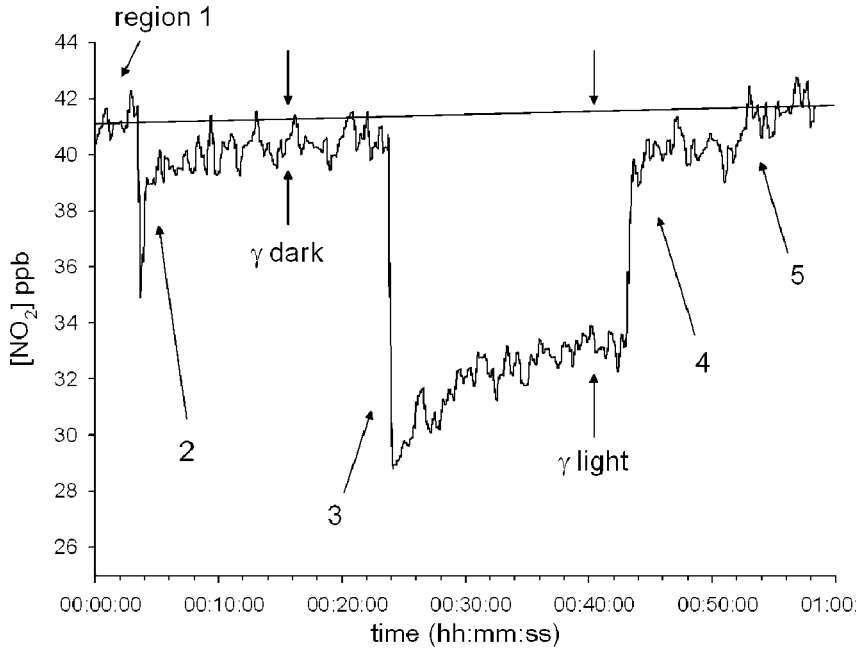

Figure 2. Results of a typical experimental run showing the NO_2 variation during the uptake experiment. The experimental steps 1−5 (see text) are indicated. At the start of the experiment, a constant NO_2 stream (41 ppb) is established (region 1); the injector is withdrawn at point 2 to expose the flow to a fresh pyrene film (18.1 μg cm^{-2}); at point 3, the lamps are turned on; at point 4, the light source was switched off; and at point 5, the injector was returned to the initial position (0 cm).

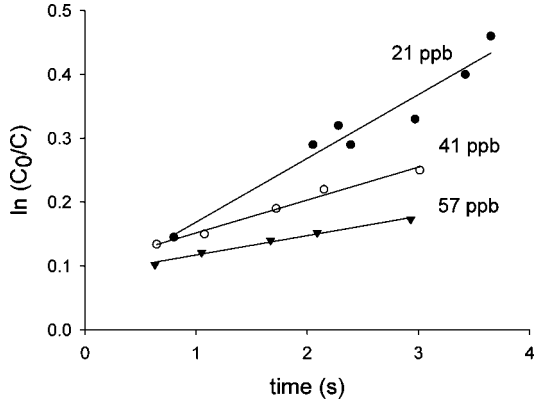

Figure 3. Loss of NO_2 as a function of exposure time to a pyrene film (18.1 μg cm^{-2}) under illuminated conditions (total flux of 9.5 × 10^{14} photons cm^{-2} s^{-1}). The filled circles, hollow circles, and triangles correspond to 21, 41, and 57 ppbv of NO_2 present in the flow tube, respectively.

level at this stage remained constant for as long as we made measurements, for over two hours in one experiment. After some time, the steps were reversed, first switching off the lamps (point 4), then pushing the injector forward to its original position (point 5). The flow tube was then cleaned thoroughly, and a fresh pyrene sample was deposited for the subsequent experiment

As shown in Figure 3, the measured loss as a function of exposure time (length) can be well fit by assuming a first-order process with respect to the gas-phase concentration of NO_2. The derived first-order rate coefficient, k_{obs}, is related to the uptake coefficient (γ) by

$$k_{obs} = \frac{d}{dt} \ln \frac{C_0}{C} = \frac{\gamma \langle c \rangle}{2 r_{tube}} \quad \text{(I)}$$

where r_{tube}, γ and $\langle c \rangle$ are the flow-tube radius ($r_{tube} = 0.55$ cm), uptake coefficient, and average molecular velocity, respectively, and C_0 and C give the NO_2 concentrations in the absence and presence of reaction (i.e., shown in Figure 2 as region 1 and dark uptake), respectively. The uptake coefficient is a phenomenological quantity, defined as the fraction of collisions which a gas-phase reagent makes with a surface which result in the net loss of that reagent from the gas phase. Equation I does not account for possible diffusion limitations caused by a radial gradient in the gas concentrations which could occur if the loss at the surface is faster than gas-phase diffusion replenishes the near-surface regime. To correct the measured uptake coefficients for gas-phase diffusion, we used the Cooney−Kim−Davis method.[28,29] The diffusion coefficient D was calculated by using the formula proposed by Fuller et al.[30] and molecular diffusion volumes of 16.76 cm^3 mol^{-1} for NO_2 and 18.5 cm^3 mol^{-1} for N_2. The correction was between 3 and 6%, with the larger corrections required for the largest uptake rates. The final values of γ reported here were assigned experimental uncertainties primarily due to the precision on multiple k_{obs} determinations (at the 2σ level). There is some asymmetry in the uncertainties because of the higher diffusion corrections applied to the higher loss rates.

Results

The most significant results of these experiments are shown in Figure 4, which illustrates the uptake coefficients determined in dark and light conditions as a function of NO_2(g) concentration. In the dark experiments, shown as hollow symbols, the uptake coefficient is small and decreases by about a factor of 4 (from 2.3 × 10^{-7} to 5.8 × 10^{-8}) over the range 20−119 ppbv of NO_2(g). The solid symbols show the result under illumination, where the uptake coefficients are an order of magnitude greater and also decrease with increasing NO_2(g) concentration, from 3.5 × 10^{-6} at 20 ppbv to 6.0 × 10^{-7} at 119 ppbv of NO_2. In each case, the curves drawn through the points show fits of the data to an inverse function of the NO_2 abundance (vide infra).

No dependence of the uptake coefficient on the amount of pyrene deposited on the walls of the flow tube was observed over the surface density range 0.2−36 μg cm^{-2}, corresponding

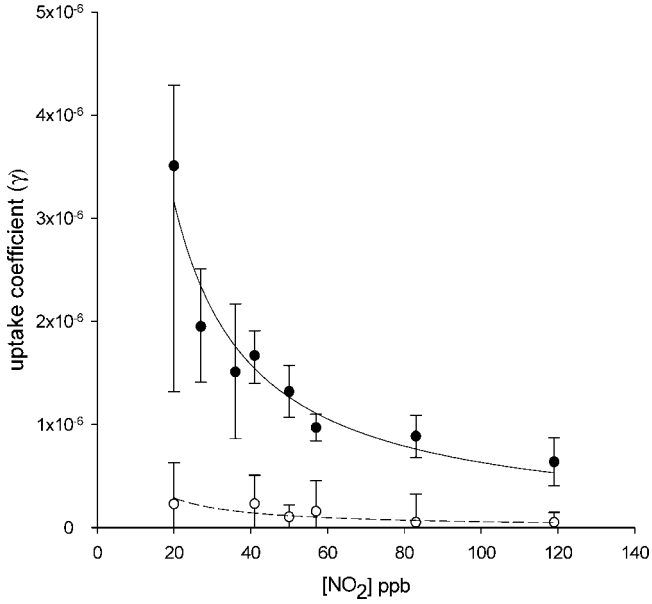

Figure 4. Uptake coefficients for NO_2 onto solid pyrene films as a function of the initial NO_2 gas concentration The filled circles show results from the irradiated experiment, and the empty circles represent uptake in dark conditions. In each case, the lines show fits of the data to an inverse function of $[NO_2]$, as implied by the Langmuir−Hinshelwood mechanism.

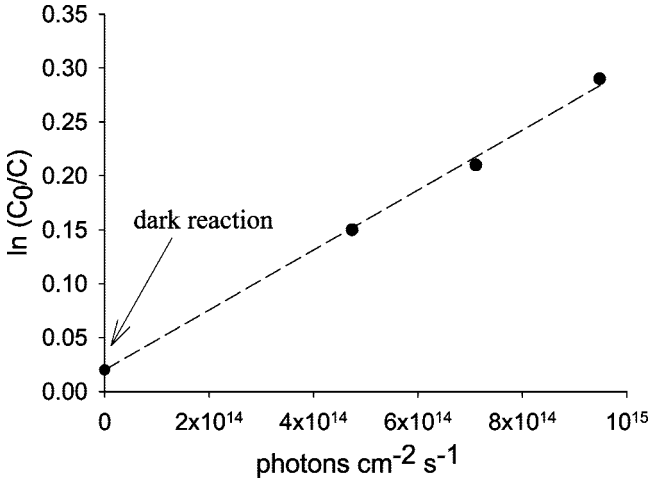

Figure 5. Effect of irradiation intensity on the NO_2 consumption for a contact time of 2.05 s. The dashed line is a linear fit to the data, and the point at zero irradiance shows the result under dark conditions.

to an estimated thickness of 4−50 molecular layers of pyrene. As well, within the error estimates, we see no clear dependence of the uptake on RH between 10 and 90%, for either dark or illuminated conditions, at least at 283 K. These results are displayed as Figures S1 and S2, respectively, in the Supporting Information.

Figure 5 shows the loss of NO_2(g) as a function of the total irradiance, which was varied by changing the number of lamps which were allowed to illuminate the pyrene sample. A clear linear dependence of the nitrogen dioxide loss on the intensity of illumination is seen, with an intercept which is identical to the uptake coefficient measured under dark conditions.

Gas-phase HONO and NO products were detected under the same illuminated conditions which gave rise to enhanced NO_2 uptake, as displayed in Figure 4. We estimate that ∼15% of the NO_2 loss is accounted for by HONO production, and a further ∼30% yields NO. There is significant uncertainty associated with quantifying the yields because of the subtractions involved in their determination; we estimate a factor of 2 uncertainty in each. Within this uncertainty, the yields are independent of the initial NO_2 concentration over the range 60−200 ppbv.

Discussion

The results may be summarized as follows: in the dark, gas-phase NO_2 exhibits a small uptake coefficient onto films of solid pyrene, perhaps with a weak inverse dependence on the NO_2 partial pressure. Under near-UV illumination, the uptake coefficient increases by an order of magnitude (depending on the illumination intensity) and shows a clear inverse dependence on the NO_2 partial pressure, consistent with a Langmuir−Hinshelwood kinetic mechanism. About 50% of the NO_2 loss under illumination gives rise to formation of the gas-phase products HONO and NO. The photoenhancement of the uptake is linearly dependent on the irradiance. The results do not depend upon the thickness of the pyrene film under either dark or illuminated conditions, consistent with a loss process involving only the outermost layers of pyrene. There is no discernible dependence of the uptake coefficient on the RH, over the range 10−90%.

NO_2 absorbs light in the wavelength region spanned by the lamps and dissociates with unit quantum yield following absorption of radiation shorter than 400 nm wavelength. An estimate of the photolysis rate constant for gas-phase NO_2 under our illumination conditions suggests that direct photolysis could give rise to a loss of at most a few percent of the total NO_2(g). Inspection of the data in Figure 2 indicates that this amount of loss is small compared to that measured here. We conclude that the photoenhancement of the uptake coefficient under illuminated conditions is not primarily due to gas-phase photolysis of NO_2 by the lamps. This conclusion is also indicated by the dependence of γ on the NO_2 concentration: for direct photolysis, there should be no concentration dependence of the first-order loss rate of nitrogen dioxide, contrary to what is observed. This dependence of γ on $[NO_2(g)]$ also argues against the reaction of NO_2*(g) with the solid film, where again, no concentration dependence is expected. A similar calculation of the photolysis rate for HONO(g) in the reactor indicates that the NO product we observe is not due to HONO photodissociation in the gas phase.

The heterogeneous reaction kinetics of NO_2 with pyrene- (as well as other PAH) coated particles in the dark has been reported.[16,17] In those experiments, the loss rate of pyrene was determined on different substrates for single, atmospherically relevant partial pressures of NO_2. Products were not identified, but the loss rate did seem to depend on the nature of the substrate upon which the pyrene was deposited. In the only other recent experiment to measure loss of the gas-phase reagent, Gross and Bertram[8] reported an upper limit to the uptake coefficient of 100 ppbv of gaseous NO_2 on solid pyrene to be 1.4×10^{-6}, consistent with the results reported above and displayed as the hollow circles in Figure 4.

In common with dark reactions of ozone with surface-associated PAH compounds, we find an inverse dependence of the uptake coefficient with NO_2 concentration under illuminated conditions. As illustrated in Figure 4, although this dependence is quite clear for the uptake under illumination, it is much less obvious under dark conditions. Given the very small values and large uncertainties measured for γ in the dark, it is difficult to draw an unambiguous conclusion concerning its dependence on $[NO_2(g)]$. We do note, however, that the quality of the fit to an inverse function is quite superior to that obtained by assuming

no dependence on the amount of [NO_2(g)] ($r^2 = 0.66$ vs 0.16, respectively). If there is indeed no dependence of γ on [NO_2(g)], we determine its value to be $(1.3 \pm 0.8) \times 10^{-7}$ over the range of NO_2 abundances explored here.

An inverse dependence of the uptake coefficient on the gas-phase reagent concentration was noted first in the reaction of ozone with benzo[*a*]pyrene adsorbed onto soot[15] and has been reported for several other systems since then.[11,12,31] This behavior is consistent with a Langmuir−Hinshelwood kinetic mechanism, in which the gas-phase reagent partitions between gas and surface, and reaction takes place between the two adsorbed species. As described in Pöschl et al.,[15] this mechanism gives rise to an inverse dependence of the uptake coefficient on the gas-phase concentration.

We note that the present results, although suggestive of such a surface-mediated kinetic mechanism, may also be interpreted as a direct reaction of the gas-phase NO_2 with the electronically excited pyrene film. Rapoport et al.[32] and more recently Emeline et al.[33] show that for heterogeneous photocatalysis reactions, a Langmuir−Hinshelwood-type dependence of the pseudofirst order heterogeneous reaction rate on the gas-phase reagent concentration may be obtained in the absence of the adsorptive step required in the Langmuir−Hinshelwood picture. Although both of the two mechanisms would predict the same dependence on [NO_2(g)], the short lifetime (∼50 ns) of excited pyrene films under nitrogen[34] argues somewhat against the direct mechanism. As well, if the dark reaction does proceed via a Langmuir−Hinshelwood mechanism, it implies that NO_2 will partition to the surface, and therefore, the same mechanism could hold under illumination as well.

As expected, the amount of photoenhancement depends linearly on the light flux reaching the reactor walls, as shown in Figure 5. The degree of enhancement observed under full illumination—about an order of magnitude—is significantly larger than that reported for the reaction with anthracene under the same illumination conditions,[22] which amounted to approximately a factor of 2. This is likely due to the greater degree of overlap between the lamp output and the pyrene absorption spectrum than with the anthracene absorption, which is significantly less intense in the 320−400 nm region. This observation also argues against a reaction involving photoexcited adsorbed NO_2* and the ground-state pyrene substrate, because the production of NO_2* should be similar in the two experiments and anthracene is more reactive toward (ground-state) NO_2 than pyrene.[17,35]

It is interesting to note that there is no apparent influence of humidity on the uptake coefficients measured either in darkness or light. Adsorbed water, present at higher RHs, was found to inhibit the reaction of ozone with benzo[*a*]pyrene on soot surfaces.[15] This was interpreted as being due to competition between water and ozone for adsorptive sites on the soot surface. However, NO_2 hydrolyses on solid or aqueous surfaces, yielding HONO and nitric acid as products, suggesting that adsorbed water might promote uptake. Under our driest conditions, there may remain one or two monolayers of water on the solid pyrene film; therefore, we cannot completely rule out this process from being responsible for the observed uptake. However, one would expect more water to be present (and therefore, perhaps, more rapid hydrolysis) at the higher RHs; nevertheless, there is no enhancement (within our uncertainties) in the uptake under these conditions.

Consistently with this, Perraudin et al.[17] conclude that reaction of water vapor coadsorbed with PAHs on silica particles was negligible under their experimental conditions. Ramazan et al.[36] do report a photoenhancement of HONO production during the heterogeneous hydrolysis of NO_2 on glass surfaces. However, they attribute this to photolysis of the nitric acid product and state that the heterogeneous hydrolysis (i.e., reactive uptake) of NO_2 is not itself photoenhanced. Arens et al.[21] studied the dark reaction between NO_2 and solid anthrarobin (1,2,10-trihydroxy-anthracene) and found that both NO_2 uptake and HONO formation increased with increasing RH. The presence of adsorbed water was postulated to promote hydrolysis of the hydroxyl groups of the substrate, which then became reactive toward NO_2. However, pyrene does not contain any functional groups which could be activated by the presence of water.

The results presented above imply that the uptake under illumination is a consequence of a heterogeneous reaction of nitrogen dioxide with the photoexcited pyrene film. Solid pyrene shows similar absorption to the molecule, but its fluorescence spectrum indicates excimer formation in the excited state.[37] (See Figure S3 in the Supporting Information for an illustration of this). Photoexcited pyrene has been reported to reduce metal ions, specifically Cu^{2+} and Ag^+, in solution.[38,39] Thus, it is possible that photoexcited pyrene may reduce NO_2 to HONO and NO, which is consistent with our observation of HONO and NO yields of ∼15 and ∼30%, respectively. Additionally, there must be formation of some solid product, possibly nitro-pyrenes,[20,40] via reaction of the photoexcited pyrene with adsorbed NO_2. Certainly, some such reactive loss of the pyrene is expected, given the results of Villenave and co-workers.[16,17] This expectation is not at odds with our observation that the NO_2 uptake is independent of time, at least over the course of a few hours; we estimate that under our conditions, only a few percent of the surface pyrene molecules would have reacted in this time.

Wang et al.[41] demonstrated that the nitration of pyrene (Py) in the dark by NO_2 requires an induction period, corresponding to the delay required for the formation of nitric acid from the hydrolysis of NO_2. Nitric acid may act as a catalyst, because the formation of electrophiles depends on the availability of H^+, as shown in their proposed mechanism:

$$NO_2 + H^+ \rightarrow HNO_2^+ \quad \text{(R1)}$$

$$HNO_2^+ + Py \rightarrow [Py\text{-}HNO_2]^+ \quad \text{(R2)}$$

$$[Py\text{-}HNO_2]^+ + NO_2 \rightarrow Py\text{-}NO_2 + NO_2 + H^+ \quad \text{(R3)}$$

Similarly, Pryor et al.[42] investigated the nitration of different PAHs in dichloromethane and concluded that the reactions proceed through an electron transfer mechanism, in which the PAH is first converted into the PAH radical cation (PAH^+) via an electron transfer to NO_2, followed by the formation of a complex between the cation and NO_2, and finally nitration through the decomposition of the complex, that is,

$$PAH + NO_2 \rightarrow PAH^+ + NO_2^- \quad \text{(R4)}$$

$$PAH^+ + NO_2^- \rightarrow [PAH^+ - NO_2^-] \quad \text{(R5)}$$

$$[PAH^+ - NO_2^-] \rightarrow PAHNO_2 \quad \text{(R6)}$$

However, this mechanism was ruled out for reaction in the ground electronic state by considering the relevant redox potentials.[43,44] However, a type I (electron transfer) mechanism, in which a pyrene cation radical is produced by electron transfer from its excited state to oxygen, was postulated to explain the photodegradation of pyrene in water;[45] this was later also postulated to explain the photochemistry of pyrene adsorbed on silica.[46] This suggests that electron transfer from an

electronically excited state of pyrene to NO_2 could allow a mechanism similar to reactions R4–R6 and would give rise to the photonitration of pyrene. The NO product could be formed in this mechanism as well, through photolysis of the NO_2^-.

Conclusions

We have measured the uptake coefficient for NO_2 loss on films of solid pyrene over a range of gas-phase concentrations and atmospherically relevant conditions. Under near-UV illumination, the uptake coefficient depends inversely on the NO_2(g) concentration, implying a Langmuir−Hinshelwood kinetic mechanism; this mechanism may also hold in the dark. An enhancement of about an order of magnitude is seen in the uptake coefficients under illuminated versus dark conditions. No discernible dependence on the RH is observed (at least down to 10% RH), suggesting that the loss of NO_2 is not entirely due to heterogeneous hydrolysis reactions. By analogy to similar results on other organic films, we propose that pyrene acts as a photoreducing agent, producing HONO upon reaction of the illuminated pyrene film with NO_2.

Acknowledgment. C.G. acknowledges EUCAARI for a postdoctoral fellowship provided to M.B. D.J.D. thanks the European Science Foundation for the award of an exchange grant through the INTROP scientific programme. We thank Sarah Styler for providing the spectra shown in Figure S3 in the Supporting Information.

Supporting Information Available: This material is available free of charge via the Internet at http://pubs.acs.org.

References and Notes

(1) Rudich, Y. *Chem. Rev.* **2003**, *103*, 5097.
(2) Diamond, M. L.; Gingrich, S. E.; Fertuck, K.; McCarry, B. E.; Stern, G. A.; Billeck, B.; Grift, B.; Brooker, D.; Yager, T. D. *Environ. Sci. Technol.* **2000**, *34*, 2900.
(3) Gingrich, S. E.; Diamond, M. L.; Stern, G. A.; McCarry, B. E. *Environ. Sci. Technol.* **2001**, *35*, 4031.
(4) Lam, B.; Diamond, M. L.; Simpson, A. J.; Makar, P. A.; Truong, J.; Hernandez-Martinez, N. A. *Atmos. Environ.* **2005**, *39*, 6578.
(5) Simpson, A. J.; Lam, B.; Diamond, M. L.; Donaldson, D. J.; Lefebvre, B. A.; Moser, A. Q.; Williams, A. J.; Larin, N. I.; Kvasha, M. P. *Chemosphere* **2006**, *63*, 142.
(6) Donaldson, D. J.; Mmereki, B. T.; Chaudhuri, S. R.; Handley, S.; Oh, M. *Faraday Discuss.* **2005**, *130*, 227.
(7) Kahan, T. F.; Kwamena, N.-O. A.; Donaldson, D. J. *Atmos. Environ.* **2006**, *40*, 3448.
(8) Gross, S.; Bertram, A. K. *J. Phys. Chem. A* **2008**.
(9) Kwamena, N. O. A.; Earp, M. E.; Young, C. J.; Abbatt, J. P. D. *J. Phys. Chem. A* **2006**, *110*, 3638.
(10) Kwamena, N. O. A.; Staikova, M. G.; Donaldson, D. J.; George, I. J.; Abbatt, J. P. D. *J. Phys. Chem. A* **2007**, *111*, 11050.
(11) Kwamena, N.-O. A.; Thornton, J. A.; Abbatt, J. P. D. *J. Phys. Chem. A* **2004**, *108*, 11626.
(12) Mmereki, B. T.; Donaldson, D. J. *J. Phys. Chem. A* **2003**, *107*, 11038.
(13) Mmereki, B. T.; Donaldson, D. J.; Gilman, J. B.; Eliason, T. L.; Vaida, V. *Atmos. Environ.* **2004**, *38*, 6091.
(14) Perraudin, E.; Budzinskia, H.; Villenave, E. *J. Atmos. Chem.* **2007**, *56*, 57.
(15) Pöschl, U.; Letzel, T.; Schauer, C.; Niessner, R. *J. Phys. Chem. A* **2001**, *105*, 4029.
(16) Esteve, W.; Budzinski, H.; Villenave, E. *Atmos. Environ.* **2006**, *40*, 201.
(17) Perraudin, E.; Budzinskia, H.; Villenave, E. *Atmos. Environ.* **2005**, *39*, 6557.
(18) Mak, J.; Gross, S.; Bertram, A. K. *Geophys. Res. Lett.* **2007**, 34.
(19) Adamson, A. W.; Gast, A. P. *Physical Chemistry of Surfaces*; John Wiley & Sons, Inc.: New York, 1997.
(20) Pitts, J. N.; Vancauwenberghe, K. A.; Grosjean, D.; Schmid, J. P.; Fitz, D. R.; Belser, W. L.; Knudson, G. B.; Hynds, P. M. *Science* **1978**, *202*, 515.
(21) Arens, F.; Gutzwiller, L.; Gäggeler, H. W.; Ammann, M. *Phys. Chem. Chem. Phys.* **2002**, *4*, 3684.
(22) George, C.; Strekowski, R. S.; Kleffmann, J.; Stemmler, K.; Ammann, M. *Faraday Dicuss.* **2005**, *130*, 195.
(23) Gustafsson, R. J.; Orlov, A.; Griffiths, P. T.; Cox, R. A.; Lambert, R. M. *Chem. Comm.* **2006**, 3936.
(24) Jammoul, A.; Gligorovski, S.; George, C.; D'Anna, B. *J. Phys. Chem. A* **2008**, *112*, 1268.
(25) Stemmler, K.; Ammann, M.; Donders, C.; Kleffmann, J.; George, C. *Nature* **2006**, *440*, 195.
(26) Stemmler, K.; Ndour, M.; Elshorbany, Y.; Kleffmann, J.; D'Anna, B.; George, C.; Bohn, B.; Ammann, M. *Atmos. Chem. Phys.* **2007**, *7*, 4237.
(27) Gutzwiller, L.; George, C.; Rössler, E.; Ammann, M. *J. Phys. Chem. A* **2002**, *106*, 12045.
(28) Cooney, D.; Kim, S.; Davis, E. J. *Chem. Engineer. Sci.* **1974**, *29*, 1731.
(29) Murphy, D. M.; Fahey, D. W. *Anal. Chem.* **1987**, *59*, 2753.
(30) Fuller, E. N.; Ensley, K.; Giddings, J. C. *J. Phys. Chem.* **1969**, *73*, 3679.
(31) Clifford, D.; Donaldson, D. J.; Brigante, M.; D'Anna, B.; George, C. *Environ. Sci. Technol.* **2008**, *42*, 1138.
(32) Rapoport, V. L.; Antipenko, B. M.; Malkin, M. G. *Kinet. Katal.* **1968**, *9*, 1306.
(33) Emeline, A. V.; Ryabchuk, V. K.; Serpone, N. *J. Phys. Chem. B* **2005**, *109*, 18515.
(34) Styler, S. MSc., University of Toronto, 2008.
(35) Esteve, W.; Budzinski, H.; Villenave, E. *Atmos. Environ.* **2004**, *38*, 6063.
(36) Ramazan, K. A.; Syomin, D.; Finlayson-Pitts, B. J. *Phys. Chem. Chem. Phys.* **2004**, *6*, 3836.
(37) Birks, J. B.; Kazzaz, A. A. *Proc. R. Soc. London, Ser. A* **1968**, *304*, 291.
(38) Jao, T. C.; Beddard, G. S.; Tundo, P.; Fendler, J. H. *J. Phys. Chem.* **1981**, *85*, 1963.
(39) Nakamura, T.; Kira, A.; Imamura, M. *J. Phys. Chem.* **1983**, *87*, 3122.
(40) Pitts, J. N.; Sweetman, J. A.; Ziellinska, B.; Atkinson, R.; Winer, A. M.; Harger, W. P. *Environ. Sci. Technol.* **1985**, *19*, 1115.
(41) Wang, H. M.; Hasegawa, K.; Kagaya, S. *Chemosphere* **2000**, *41*, 1479.
(42) Pryor, W. A.; Gleicher, G. J.; Cosgrove, J. P.; Church, D. F. *J. Org. Chem.* **1984**, *49*, 5189.
(43) Eberson, L.; Radner, F. *Acta Chem. Scand., Ser. B* **1985**, *39*, 343.
(44) Eberson, L.; Radner, F. *Acta Chem. Scand., Ser. B* **1985**, *39*, 357.
(45) Sigman, M. E.; Schuler, P. F.; Ghosh, M. M.; Dabestani, R. T. *Environ. Sci. Technol.* **1998**, *32*, 3980.
(46) Reyes, C. A.; Medina, M.; Crespo-Hernandez, C.; Cedeno, M. Z.; Arce, R.; Rosario, O.; Steffenson, D. M.; Ivanov, I. N.; Sigman, M. E.; Dabestani, R. *Environ. Sci. Technol.* **2000**, *34*, 415.

JP802324G